Scaling Laws for Reduced-Scale Tests of Pulse Jet Mixing Systems in Non-Newtonian Slurries: Mixing Cavern Behavior

P. A. Meyer, D. E. Kurath, J. A. Bamberger
Battelle – Pacific Northwest Division
P.O. Box 999, Richland, WA 99352
USA

S. M. Barnes
Washington Group International
2940 George Washington Way
Richland, WA 99354
USA

A. Etchells
AWE 3 Enterprises
315 S. 6th Street
Philadelphia, PA 19106
USA

ABSTRACT

The Waste Treatment Plant (WTP) under construction at the Hanford Site will use pulse jet mixer (PJM) technology for mixing and gas retention control applications in tanks expected to contain waste slurries exhibiting a non-Newtonian rheology. This paper presents the results of theoretical and experimental studies undertaken to establish a methodology for performing reduced-scale mixing tests with PJM systems in non-Newtonian fluids. A theoretical model for mixing cavern formation from steady and pulsed jets is developed and compared with data from a single unsteady jet in a yield stress simulant. Dimensional analysis is used to identify the important dimensionless parameters affecting mixing performance in more complex systems. Scaling laws are proposed based on the modeling and dimensional analysis. Experimental validation of the scaling laws governing unsteady jet mixing in non-Newtonian fluids is also presented. Tests were conducted at three scales using two non-Newtonian simulants. The data were compared nondimensionally and the important scale laws confirmed. The key dimensionless parameters were found to be the Strouhal number (which describes unsteady pulse jet mixer operation), the yield Reynolds number (which governs cavern formation due to non-Newtonian fluid behavior), and the viscous Reynolds number (which determines the flow regime and the degree of turbulence). The experimentally validated scaling laws provide the basis for reduced-scale testing of prototypic WTP mixing systems. It is argued that mixing systems developed from reduced scale testing will produce conservative designs at full scale.

INTRODUCTION

Mixing Radioactive Non-Newtonian Slurries at the Hanford Waste Treatment Plant

The U.S. Department of Energy (DOE) Office of River Protection's Waste Treatment Plant (WTP) is being designed and built to pretreat and then vitrify a large portion of the wastes in Hanford's 177 underground waste storage tanks. Concentrated high-level waste slurry in the pretreatment facility is expected to exhibit complex non-Newtonian rheology. Under flow conditions, these slurries possess a

yield stress and tend to exhibit shear thinning behavior. They also develop gel-like properties when they are at rest for a period of time, behaving much like a very weak solid characterized by a shear strength.

One of the primary concerns with non-Newtonian slurries is their propensity to retain flammable gases. Radioactive waste generates hydrogen and other gases by the processes of radiolysis and thermolysis. Gases will generally bubble out of fluids with Newtonian rheology. However, even a modest shear strength will trap gas bubbles in situ and can lead to a significant amount of retained gas in a stagnant state.[1] A sudden release of this gas could result in flammable conditions in the headspace of the tank and/or the plant ventilation system. Thus, mixing systems are required to shear the waste contents enough to allow the gas to be released more gradually in a safe and controlled manner.

Process vessels in the WTP are in so-called "black cells," where no maintenance will be available for the operating life of the plant. Pulse jet mixers (PJM) were initially planned for mixing WTP vessels because they lack moving mechanical parts that would require maintenance. A typical PJM system is illustrated in Figure 1. PJM mixing technology involves a pulse tube coupled with a jet nozzle. One end of the tube is immersed in the tank, while periodic pressure, vacuum, and venting are supplied to the opposite end. There are three operating modes for the pulse tube: 1) the drive mode, when pressure is applied to discharge the contents of the PJM tube at high velocity through the nozzle; 2) the refill mode, when vacuum is applied to refill the pulse tube; and 3) the vent mode, when the pressure is vented to atmosphere and the pulse tube and tank approach the same fill level. The PJM system uses these operating modes to produce a sequence of drive cycles that provide mixing in the vessel. PJM operating parameters—applied pressure, nozzle exit velocity, nozzle diameter, and drive time—along with the rheological properties of the fluid being mixed, all contribute to the effectiveness of mixing within the vessel. Several PJMs are typically installed in a cluster in the center of the tank such that the combined pulse tubes contain 10 to 15% of the total tank volume. The discharge velocity varies continuously during the cycle, so the mixing is intrinsically unsteady.

Unsteady Jet Mixing of Non-Newtonian Fluids
PJM technology had been used successfully for mixing Newtonian fluids in radioactive environments. However, applying the technology to non-Newtonian slurries was new with the WTP, and an adequate supporting technical basis was not available. The field of Newtonian fluid mixing is mature and supported by significant theoretical and practical knowledge for designing mixing systems. These systems can be mechanical (impellers or agitators) or hydrodynamic (steady or pulsed fluid jets). For non-Newtonian fluids, the majority of mixing experience is associated with mechanical agitators. The subject of jet mixing in non-Newtonian fluids is a relatively new and developing field, with some theoretical analysis and applied research being pursued in industry and academia. Unsteady jet mixing in non-Newtonian fluids is essentially a new topic of study.

From a hydrodynamic perspective, PJMs provide unsteady, turbulent, momentum-driven jets that impinge on the vessel floor. With non-Newtonian fluids, the primary mixing objective is to overcome the yield stress and mobilize the fluid. A common phenomenon observed in mechanical mixing of non-Newtonian fluids is the formation of a mixing cavern. The cavern is essentially a bounded region near the mixer that is highly agitated and turbulent, surrounded by material that is essentially stationary. The transition between the two regions can be very abrupt. Caverns have also been observed with steady jet mixing systems [2] as well as PJMs. This result is to be expected given the hydrodynamic similarity between jet mixing and mechanical agitation—both create fluid motion. A successful mixing system design involves placing and operating the mixers so no regions of stationary material remain in the mixing vessel. Thus a basic understanding of cavern formation is essential.

The PJM Non-Newtonian Test Program

The WTP undertook a comprehensive integrated test program to evaluate prototypic mixing systems designs at reduced scale.[3] The first phase of the program involved theoretical and experimental studies to establish the methodology and technical basis for reduced scale testing. This included non-Newtonian simulant development [4], theoretical treatment of mixing and gas release behavior [5, 6], identifying appropriate scaling laws, and verifying the scaling laws experimentally.[5, 6] Later phases of the program involved scaled tests of prototypic systems and eventually evolved into testing PJM-hybrid mixing systems.[7]

This paper describes the research conducted to develop and validate scaling laws that can be applied to scaled tests of pulse jet mixing in non-Newtonian slurry. The focus is limited to mixing behavior, with gas retention and release behavior treated in a companion paper. As a starting point, a simple theoretical model for cavern formation from a single PJM is presented. The important dimensionless parameters governing cavern formation are discussed, and a scaling methodology is presented. Results of testing of 4-PJM systems with two different non-Newtonian simulants are presented.
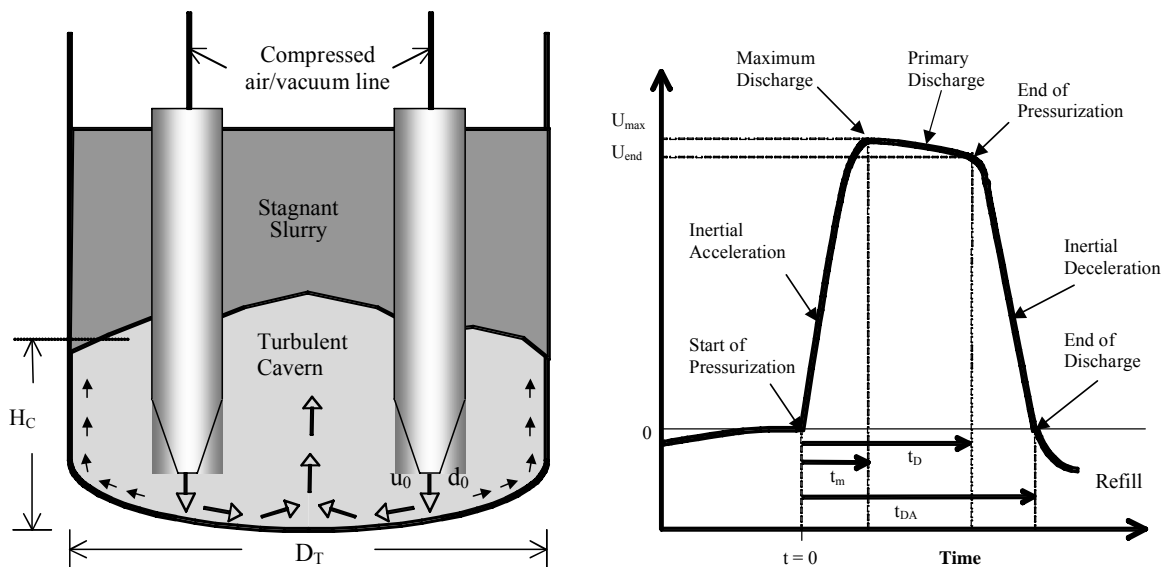

Fig. 1. Illustration of a typical pulse jet mixing system. On the left is a mixing cavern in a non-Newtonian slurry; the right shows the temporal variation of discharge velocity.

CAVERN FORMATION FROM UNSTEADY JETS

Assumptions
Cavern formation from operating pulse jet mixers in non-Newtonian slurries is a complex phenomenon. The non-Newtonian rheology, the behavior of the unsteady non-Newtonian jets, and the geometry of the mixing system and vessel must be considered. The modeling strategy used simplifying assumptions that make the problem tractable while retaining the first-order essential characteristics of the physical phenomena. A brief discussion of some of the important assumptions and simplifications follows.

Rheology: Laminar flow rheograms of actual waste samples suggest the waste behaves approximately like a Bingham plastic, characterized by yield stress, τ_y, which is the shear stress extrapolated to zero strain rate, and consistency, κ, the slope of the linear region. The bounding best-fit parameters of actual waste slurry are $\tau_y = 30$ Pa and $\kappa = 30$ cP. While the Bingham plastic assumption is useful and fairly simple, it does not adequately describe all the relevant rheology for the cavern formation problem. Before

it is disturbed, actual waste slurry will possess shear strength, τ_s, that is typically much higher than the Bingham yield stress. Thus, the actual waste appears to be thixotropic; i.e., the shear stress can decrease while experiencing a strain rate. Because the time required for the shear strength to develop again is longer than the cycle time of the PJMs, it is assumed the slurry within the mixing cavern is adequately characterized by the yield stress, while the slurry outside the cavern is characterized by the shear strength. One limitation of the Bingham plastic model is that turbulent conditions exist inside the cavern. The behavior of Bingham plastic fluids in turbulent flow is not well understood. The yield stress may not be present (or significant) for turbulent flow of a particulate slurry. Rather, the behavior is more Newtonian, with the Newtonian viscosity (μ) approximately equal to Bingham consistency (κ). However, the Bingham yield stress may be important in the boundary layer at the cavern interface. As the velocity slows at the interface, it will at some point re-laminarize, and Bingham rheology will apply. Overall, it is expected that the shear strength, τ_s, yield stress, τ_y, and consistency, κ, are the most important rheological parameters governing cavern formation in particulate-laden, non-Newtonian slurry.

Jet Behavior: The behavior of Newtonian jets is primarily determined by geometry and the jet Reynolds number, $Re_0 = \rho u_0 d_0 / \mu$. Non-Newtonian rheology is expected to affect the structure and decay of turbulent jets. However, if the jet Reynolds number is large the jet will be highly turbulent, and rheology should not have a dominant effect. For modeling purposes, we assume the jet behaves like a turbulent Newtonian jet, with self-similar velocity profiles. Unsteady jet effects are handled by making a quasi-steady assumption that steady jet velocities exist at a given instant, and vary in time with the variation in discharge.

Geometry: The PJM systems to be used in the WTP involve multiple pulse tubes arranged at various radial locations in a given vessel. For modeling purposes we consider the single PJM system, so any three-dimensional or jet interaction effects are not treated. Further, the shape of the vessel bottom likely affects the behavior of the impinging jets and hence the mixing cavern. The model assumes flat-bottom vessels.

A Simple Model for Cavern Height

The model begins with the consideration of a basic turbulent jet. Three-dimensional, steady, turbulent jets, whether free (away from boundaries) or impinging on boundaries, are known to follow the similarity law [8]:

$$u(z) = c_J \frac{u_0 d_0}{z} \qquad \text{(Eq. 1)}$$

where z is the distance to any point along the primary path of the jet, u(z) is the maximum time-averaged velocity at point z, and c_J is a constant accounting for the effects of geometry. The value of c_J for Newtonian turbulent circular free jets is known to be a weak function of the jet Reynolds number [9] and is typically in the range ~5 to 6.

To apply Eq. (1) to an unsteady jet created by a PJM, the discharge velocity, u_0, must be defined by some suitable average. The velocity varies spatially over the cross section of the nozzle and temporally in response to varying drive pressure and inertia. Various averaging approaches were considered for the transient velocity profiles (illustrated in Fig. 1). The averaging approach that ultimately provided the best correlation of test data was the "peak average" velocity, defined by

$$u_0 = \frac{1}{t_D - t_m} \int_{t_m}^{t_D} u \, dt \qquad \text{(Eq. 2)}$$

where t_D is the time for which the primary drive pressure is applied, t_m is the time at which the maximum velocity occurs, and u is instantaneous velocity at t_m. The actual drive time, t_{DA}, is greater than t_D due to the inertia of the slug of fluid inside the PJM and the finite vent time of the system.

We assume that Eq. (1), together with the jet velocity given by Eq. (2), describes the decay of the jet as it spreads radially along the bottom and then moves up the wall of the vessel. This decaying jet will produce fluid stress along solid boundaries. For turbulent Newtonian flows, the fluid stress can generally be expressed as

$$\tau_f = C_f \frac{1}{2}\rho u^2 \qquad \text{(Eq. 3)}$$

where u is the local average velocity, ρ is the fluid density, and C_f is the stress coefficient, which is a function of jet Reynolds number. If the cavern interface behaves essentially as a solid "wall," the resultant fluid stress must balance the strength of the undisturbed slurry when the jet reaches height H_c (the top of the cavern illustrated in Fig. 1). Hence by equating Eq. (3) to the shear strength (within a constant of proportionality) and evaluating Eq. (1) at the cavern boundary ($z \approx H_C + D_T/2$), the following expression for normalized cavern height is obtained:

$$\frac{H_C}{D_T} = a\frac{d_0}{D_T}Re_\tau^{1/2} - \frac{1}{2} \qquad \text{(Eq. 4)}$$

where the yield Reynolds number $Re_\tau = \rho u_0^2 / \tau_s$ has been introduced and the coefficient, a, is in general a function of jet Reynolds number. The yield Reynolds number is essentially the ratio of jet dynamic pressure to material shear strength. Equation (4) suggests that the normalized cavern height resulting from a single downward impinging steady jet increases linearly with nozzle diameter and the square root of the yield Reynolds number.

To address unsteady effects associated with pulse jet operation, the theory can be modified by introducing the flow establishment time, t_{SS}. A real jet requires a finite time to establish steady-state flow conditions. The magnitude of the unsteady effect depends upon the ratio of pulse jet drive time to the flow establishment time. The flow establishment time can be approximated as a particle transit time from the nozzle to the cavern interface and can be obtained by integration of Eq. (1). The drive time can be written in terms of the volume of fluid discharged during a pulse, V_P. Hence, the ratio of the two time scales is found to be

$$\frac{t_D}{t_{ss}} \sim \frac{V_P}{d_0^3 Re_\tau} \qquad \text{(Eq. 5)}$$

When the drive time is short relative to the flow establishment time, unsteady effects dominate. If the drive time is large compared with flow establishment time, the flow behaves essentially like a steady jet. The resulting expression for cavern height after including the unsteady jet effect is given by

$$\frac{H_C}{D_T} = b\frac{d_0}{D_T}Re_\tau^{1/2}\left(1-\exp(-c\frac{V_P}{d_0^3 Re_\tau})\right)^{1/2} - \frac{1}{2} \qquad \text{(Eq. 6)}$$

where b and c are weak functions of the jet Reynolds number. If the ratio of drive time to flow establishment time is very large, Eq. (6) limits the steady jet result given by Eq. (4). For all finite values of the ratio, the cavern height is reduced.

Figure 2 compares the cavern height predicted by Eq. (6) and results of cavern formation experiments with steady and pulsed jets. Laponite, a transparent gel-like material that develops shear strength in the range of 10–150 Pa, was used as the simulant. Tests were conducted with a 2.5-cm nozzle (for 31-Pa shear strength tests) and a 5.1-cm nozzle (for 44-Pa shear strength tests). The pulse volume, V_P, was 0.018 m^3 for the 2.5-cm nozzle test and 0.032 m^3 for the 5.1-cm nozzle test. Also shown are data from a steady jet test with a 2.2cm nozzle in 44Pa Laponite. Excellent agreement is seen between the data and theoretical prediction (Eq. 6 with the value of b = 1.67 and c = 1.4).
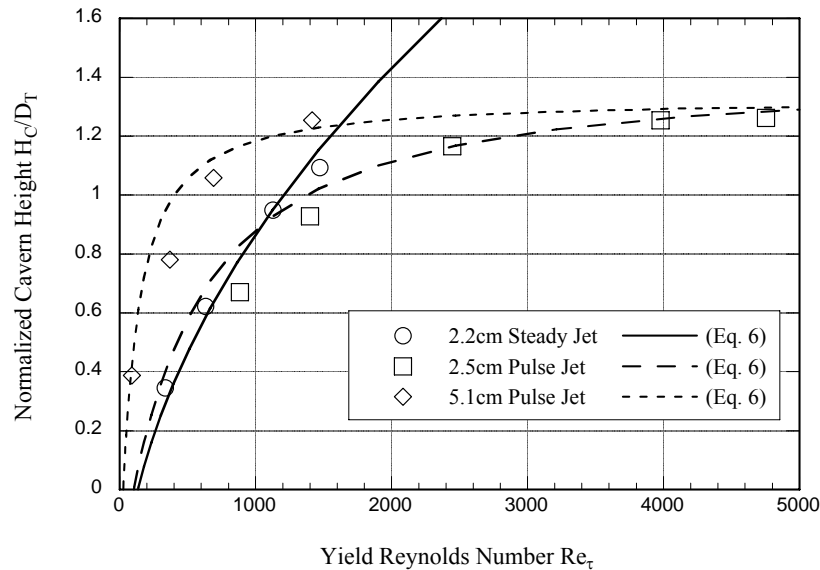

Fig. 2. Theoretical prediction of cavern height for a single pulse jet compared with Laponite data; steady jet data also shown for comparison

Multiple PJM Systems
The model for cavern height applies to a single PJM centered in a cylindrical flat-bottomed vessel. WTP vessels are cylindrical and have elliptical bottoms and multiple PJMs. Typically, six or eight PJMs are arranged symmetrically in the vessel. One difference between single and multiple PJM mixing systems is a strong central upwelling flow. While the jets impinge on the elliptical bottom, a significant fraction of the flow moves radially inward and turns up at the center of the tank. The central upwelling can lead to potential breakthrough at the surface, leaving an annulus of stationary slurry in the upper region of the vessel. The functional dependence of physical parameters illustrated by the single PJM theory should apply to the multiple PJM configuration. The primary difference, the effective nozzle diameter, is given by $d_{0e} = c\sqrt{N}d_0$, where N is the number of PJMs and c is a constant determined by geometry. Because the primary flow is upward, it is likely that the cavern interface will be dominated by the normal stress of the jet as opposed to the shear stress. Because normal fluid stress is always larger than fluid shear stress, cavern height should be greater than Eq. (6) suggests. Once breakthrough has occurred, the basic model for cavern height will likely fail to predict subsequent cavern behavior because increases in jet velocity may increase the diameter of the breakthrough region, D_c. The dominant flow at this point may behave more like a confined flow than a jet.

SCALING LAWS

Small-scale testing is a common approach used successfully in the many fields of applied fluid dynamics. The success of the approach relies greatly on the fact that system performance depends on certain dimensionless groupings of physical parameters. If these parameter groupings can be preserved at large and small geometric scales, the essential behavior of the system will be the same at both. This principle is referred to as *similarity* in the theory of fluid dynamics engineering. Limitations of scaled testing are attributed to the inability to match important dimensionless parameter groupings at both scales. In complex fluid dynamic problems, there can be many dimensionless parameter groups; however, often the essential behavior of the phenomenon is dominated by just a few key groups. In this situation, small-scale testing can produce results that closely replicate large-scale behavior.

Dimensionless Physical Parameters
Slurry properties and PJM system parameters can be used to form dimensionless groups that dictate how scaled tests should be designed and operated to provide meaningful results. Some of these appear naturally in the mathematical model by virtue of the physical laws involved. Others can be identified by dimensional analysis or experience. This section summarizes the most important dimensionless parameters thought to influence PJM mixing behavior. A more comprehensive development is given in.[6]

The following dimensionless groups relate directly to PJM mixing. Many of them also have an indirect effect on gas retention and release behavior because the rheological state of the slurry depends on the degree of mixing. Dimensionless groups relating strictly to gas behavior are addressed in a companion paper that discusses gas retention and release.

Yield Reynolds number: $\qquad \mathrm{Re}_\tau = \dfrac{\rho u_0^2}{\tau_s}$

The yield Reynolds number is the ratio of dynamic stress to slurry strength, which directly affects the size of the mixing cavern. The yield Reynolds number can also be formed with the Bingham yield stress in the denominator.

Jet Reynolds number: $\qquad \mathrm{Re}_0 = \dfrac{\rho u_0 d_0}{\kappa}$

The jet Reynolds number is the ratio of dynamic stress to viscous stress. It affects the degree of turbulence in the mixed region as well as transitional flow regimes associated with unsteady mixing. It also affects the stress at the cavern (hence cavern height) and the thickness of boundary layers at the vessel wall.

Strouhal number: $\qquad S_0 = \dfrac{t_D u_0}{d_0}$

The Strouhal number is the ratio of pulse time to jet flow time scale. It affects the degree to which the jet approaches steady behavior. In the limit of steady jet flows the Strouhal number becomes infinite, and the effects of pulsation are no longer present. For small Strouhal numbers, the mixing behavior is highly dominated by pulsation effects.

Additional dimensionless groups can be formed from the physical parameters of the system (for example, densimetric Froude number, Deborah number etc.). However, the particulate slurries under consideration tend to have uniform density and exhibit minimal elastic behavior; hence these parameters would have only a very minor effect, if any. Other parameter groups are sometimes used in the literature that are a combination of the yield Reynolds number and jet Reynolds number. For example,

Yield number:
$$Y = \frac{\tau_s d_0}{\kappa u_0} = Re_0 / Re_\tau$$

Hedstrom number:
$$He = \frac{\rho \tau_s d_0^2}{\kappa^2} = Re_0^2 / Re_\tau$$

In general, for a given non-Newtonian PJM mixing test, any dimensionless mixing characteristic (such as normalized cavern height or mixing time) should depend on yield Reynolds number, jet Reynolds number, and Strouhal number. Therefore, the ideal small-scale test is one in which the dimensionless groups are the same as those at full scale. The extent to which the dimensionless parameters scale determines the success of the small-scale test approach. How tests are designed and operated is therefore subject to certain constraints.

Geometric Scaling Approach
The non-Newtonian test program used geometric scaling in which the geometric scale factor is defined by $s = L_L / L_S$, where L_L is any characteristic linear dimension of the large-scale system (such as tank diameter, nozzle diameter, and waste level). At small scale, every linear dimension, L_S, is reduced or scaled by s (i.e., $d_{0_S} = d_{0_L} / s$, $D_{T_S} = D_{T_L} / s$, $H_S = H_L / s$). Thus, the ideal small-scale test is an exact geometric miniature of the large system with all areas scaled according to $A_S = A_L / s^2$ and all volumes scaled according to $V_S = V_L / s^3$. Scale factors up to about 10 are considered acceptable in typical fluid mixing tests; that is, much of the important physics can be captured at small scale. For the non-Newtonian test program, the design of scaled prototypic vessels was limited to conservative scale factors in the range of 4 to 5 due to the immaturity of the technology and the importance of the outcome.

When testing at small scale, one must determine how to scale velocity (i.e., PJM drive velocity, u_0). One choice is to scale velocity by the scale factor. This is problematic, however, because it tends to reduce the Reynolds number by $1/s^2$ and introduce further difficulties with the scaling of time. A better choice is to keep jet velocity constant at both scales ($u_{0_S} = u_{0_L}$).

For steady jet mixing, time does not come into play. However, PJM operation is a periodic process, so the scaling of time must be addressed. If velocity is held constant and geometry scaled, it follows that all imposed time scales must be reduced at small scale. Similarly, to keep the jet discharge velocity the same while scaling pulse volume geometrically, pulse time will be reduced by the scale factor according to $t_{DS} = t_{DL} / s$. Hence the PJM drive time, refill time, and cycle time are all reduced by s at small scale.

Given the geometric scaling approach, the yield Reynolds number will be the same at both scales as long as the slurries have the same shear strength (or yield stress) and density. This is guaranteed if the same simulant is used at both scales; hence we have $Re_{\tau S} = Re_{\tau L}$.

The jet Reynolds number at small scale is reduced by the geometric scale factor, $Re_{0s} = Re_{0L}/s$. For highly turbulent conditions, this should introduce only minor differences in test results because the Reynolds numbers in both tests are quite large. For moderate turbulence or transitional flow, the effect will be larger. In general, mixing effectiveness will be diminished at lower jet Reynolds numbers; hence the loss of net effect on mixing performance should be conservative, with small-scale tests producing mixing of lower quality than full-scale performance. The jet Reynolds number can be matched at small scale by reducing the consistency or viscosity by the scale factor; however, this is difficult because it would require changing the consistency of the simulant while keeping the yield stress unchanged.

The geometric scaling approach requires all linear dimensions and time imposed times scales to be reduced by the scale factor. Hence, the scale effects cancel in the Strouhal number, and it will be the same at both scales ($S_{0S} = S_{0L}$). This implies that all unsteady and periodic effects will be adequately captured in small scale tests.

EXPERIMENTAL VALIDATION OF SCALE LAWS

Mixing tests were performed in geometrically similar vessels at three scales to validate the scaling laws. Each vessel was equipped with four PJMs. Tests were conducted using two different non-Newtonian simulants. We present a brief synopsis of the test equipment, the non-Newtonian simulants used, the types of test performed, and some of the key results below.

Test Vessels
Vessel scales are shown in Table I. A 45.4 m^3 vessel in the Pacific Northwest National Laboratory (PNNL) 336 Building was used for large-scale tests. The vessel was 3.9 m. in diameter and approximately 14.6 m. deep with a 2:1 elliptical bottom, making a working volume of about 37.9 m^3. The PJM system installed in the tank consisted of four evenly spaced cylindrical pulse tubes, 3 m. long and 0.61 m. in diameter. The bottom end was a 60º cone truncated to a 10 cm. nozzle opening. The overall height of the pulse tubes was approximately 3.7 m. The PJMs were operated with plant-type jet pump pairs using compressed air and controlled by a prototypical control system.

Table I. Vessels Used for 4PJM Scaling Tests

Vessel	Nominal Volume (m^3)	Vessel Diameter (m)	PJM Nozzle Diameter (cm)	Scale Factor (s)
336	45.4	3.88	10.1	1
APEL	0.95	0.86	2.22	4.53
SRNL	0.11	0.44	1.09	8.9

Experiments were also conducted at ~¼ scale at the Applied Processing and Engineering Laboratory (APEL) at Pacific Northwest National Laboratory (PNNL). This test stand was a geometrically scaled version of the large-scale 4PJM test stand with scale factor s = 4.53. However the scaled height was taller than the 336 test facility to enable testing at higher H/D_T ratios. A third set of tests at $^1/_9$ scale were conducted at Savannah River National Laboratory (SRNL). The SRNL 4PJM test stand [10] was also a linearly scaled version of the large-scale 4PJM setup in the 336 test facility, with s = 8.9. Both of the smaller vessels were equipped with a compressor/vacuum/receiver-tank system that supplied pressurized air and vacuum through a control manifold and solenoid-actuated valves to operate the PJMs.

The PJM system in the large-scale (336) vessel operated prototypically with drive times on the order of 5 to 10 seconds and total cycle times on the order of 60 seconds. The maximum "peak average" velocity achievable was about 12 m/s. Consistent with the geometric scaling approach outlined in the previous

section, the smaller vessels were operated with drive and cycle times reduced by the scale factor, while the peak average velocities were approximately constant with scale.

Simulants
Two nonhazardous, relatively inexpensive simulants were developed and used for testing, Laponite and kaolin-bentonite clay.[3] The simulants were selected based on limited actual waste slurry rheology measurements that indicate the WTP non-Newtonian waste stream can be represented by a Bingham plastic rheology model. The WTP specified bounding values are 30 Pa for yield stress (τ_y) and 30 cP for consistency (κ) for the Bingham plastic parameters.

Laponite is a synthetic smectite clay mineral consisting of nanoscale crystals in the form of platelets that make a transparent solution when dispersed in water due to their small particle size. Laponite was used primarily to represent the gelled conditions encountered by PJMs upon restart from idle periods. As such, the shear strength was considered the important rheological parameter. For low-strength Laponite (30 Pa shear strength) that has been fully sheared, the yield stress is essentially zero, and the material behaves like a Newtonian fluid. For higher-strength Laponite (80–120 Pa), the yield stress was typically in the 10-Pa range. The Laponite used had a density of 1000 kg/m^3, shear strength that ranged from 30 to 120 Pa, and a consistency in the 10 to 20 cP range. The clay used was a non-Newtonian Bingham plastic material designed to approximate the rheology of high-level waste sludge with a target yield stress of 30 Pa and a consistency of 30 cP. The density was 1200 kg/m^3, yield stress ranged from about 20 to 45 Pa and consistency from about 10 to 30 cP. The clay also developed shear strength when at rest. The value of shear strength typically was about 1.5 to 2 times the yield stress and developed over many hours. The shear strength for the clay was not considered important to the test results because the clay was thoroughly mixed before testing.

Cavern Mixing Tests
For this work, mixing was defined as fluid mobilization within the cavern (Fig. 3); no attempt was made to quantify the degree of turbulence within the cavern. Generally, PJM velocities varied over a range that provided useful data. Given the nondimensional nature of the scaling approach, the simulant rheological properties and PJM velocities did not need to be identical in the various test stands. However, the properties were similar, and velocities were maintained within useful and prototypic ranges. In some cases, higher-strength simulant conditions and higher velocities were used to fully exercise the range of experimental conditions for a given test. Three types of data were collected and analyzed to make non-dimensional comparisons:

- Cavern height measurements with Laponite at three vessel scales. Heights were measured at the center of the vessel using dyes and visual means.

- Breakthrough velocity measurements with Laponite and clay at three vessel scales. In these tests, the PJM velocities were gradually increased until fluid motion was observed at the liquid surface.

- Upwell velocity measurements in clay at two vessel scales (s = 1 and s = 4.5). Upward axial velocities were measured at the center of the vessel at various elevations.

The range of test conditions was selected to provide enough variation to establish a wide range of comparable data and to span full-scale plant operating conditions where possible. The approximate range of test conditions, including the key dimensionless parameters, is listed in Table II.

Cavern heights were measured using Laponite in the 336 (large scale), APEL, and SRNL 4PJM test vessels. Simulant shear strength (τ_s) and PJM velocity (u_p and u_a) were the two primary test variables.

Table II. Range of Conditions Tested in 4PJM Experiments Compared with Plant Conditions

Parameter	Symbol	Units	WTP Bounding	Test Range
Average PJM drive velocity	u_a	m/s	9	3.0–10.2
Peak average PJM drive velocity	u_p	m/s	12	3.3–12.2
PJM drive time	t_D	s	15–60	2–20
Nominal vessel batch volume	V_T	m^3	45–260	0.11–45
PJM nozzle diameter	d_0	cm	10	1–10
Slurry density	ρ	kg/m^3	1300	1000–1200
Slurry consistency	κ	cP	30	10–27
Slurry yield stress	τ_y	Pa	30	18–46
Slurry shear strength	τ_s	Pa	75 (est.)	30–125
Yield Reynolds number (based on u_p)	Re_τ		6,200	120–4,900
Jet Reynolds number (based on u_p)	Re_0		52,000	5,500–52,000
Strouhal number (based on u_p)	S_0		1800–7200	900–2400

The majority of the tests were performed with a simulant fill level of approximately $H/D_T = 0.9$. Some higher fill levels were conducted to examine the effect of artificially high caverns and premature surface breakthrough resulting from Laponite bulk fracture at smaller vessel scale. Normalized cavern heights are plotted versus yield Reynolds number in Figure 3. Linear regressions of the data are also shown on the plot to aid in scale comparison. Several surface breakthrough points are also included. The data show that normalized cavern height increases with increasing yield Reynolds number. While some scatter exists, the linear regression curves demonstrate that cavern heights are generally largest in the 336 vessel and decrease in the smaller vessels. Figure 4 includes data from higher fill levels. This was done because of the observation that Laponite often failed in discrete chunks. At small scale, as the cavern approaches the surface, a fracture could result in a higher cavern and potentially premature breakthrough. Inclusion of the higher fill level data suggests this was in fact the case because the breakthrough points for the APEL and SRNL tests are shifted considerably to higher yield Reynolds number. The general trend that normalized cavern heights become larger with increasing vessel scale supports the anticipated result that jet Reynolds number effects will produce higher caverns in larger vessels.
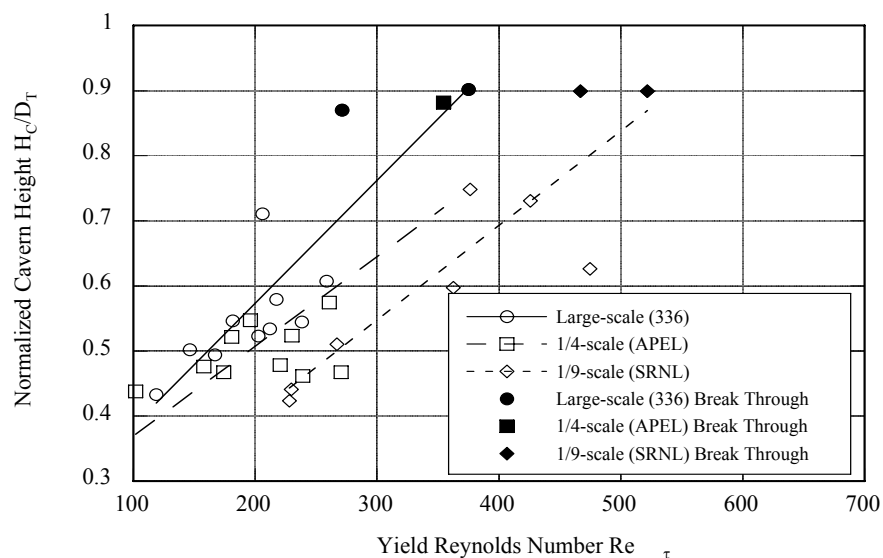

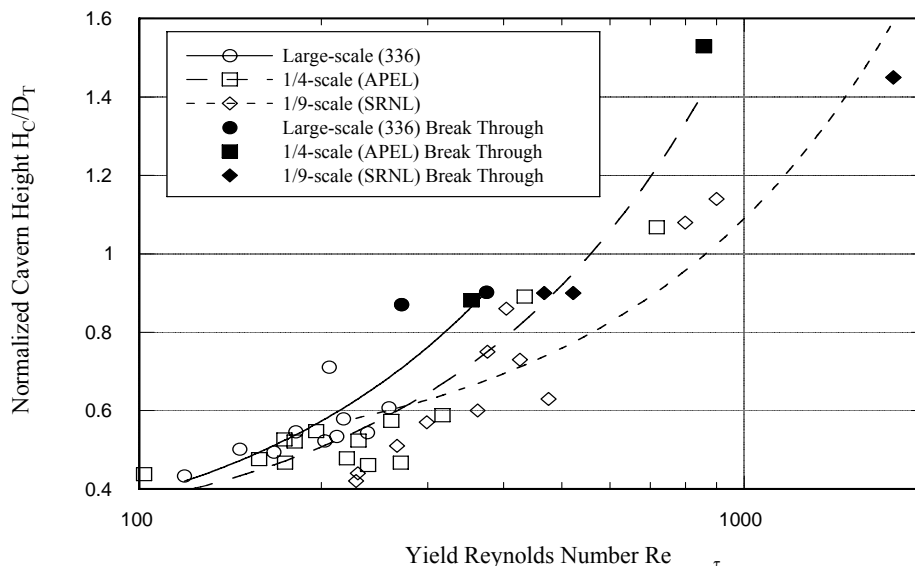Fig. 3. Normalized cavern height versus yield Reynolds number for Laponite

Fig. 4. Normalized cavern height versus yield Reynolds number,
including higher fill level data

Surface breakthrough velocities were measured using both simulants at all three scales. PJM velocities were increased until the central upwell caused the cavern to reach the surface. The specific velocity at which breakthrough occurs can be compared nondimensionally to examine the scaling relationship between the various vessel scales. Yield Reynolds numbers at breakthrough for clay and Laponite are plotted versus vessel scale factor and jet Reynolds number in Figure 5. The data clearly suggest that large vessels require a lower yield Reynolds number for breakthrough. Yield Reynolds numbers at break-through are significantly larger for clay than for Laponite. Part of this difference is attributed to the fact that shear strength in clay is about 50% higher than yield stress. However, a factor of ~5 would be required to explain the difference. This suggests that clay exhibits non-Newtonian effects on the flow structure, not just on the flow boundary, as is believed for Laponite. While there is some scatter in the
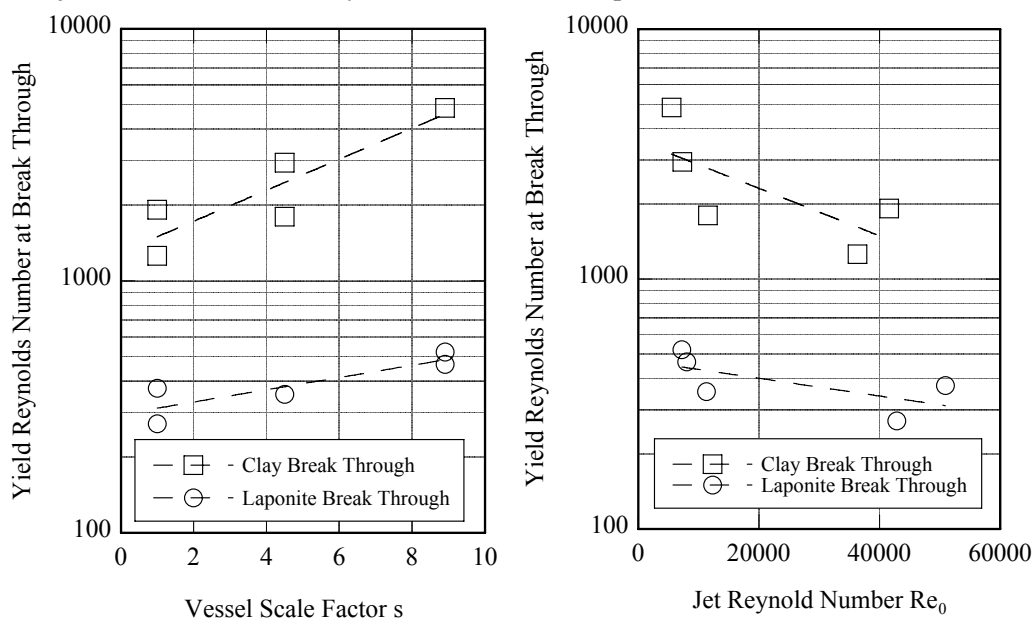

Fig. 5. Yield Reynolds number at breakthrough versus vessel scale (left)
and jet Reynolds number (right)

data, these correlations suggest that the yield Reynolds number required for breakthrough is reduced as the jet Reynolds number is increased. In physical terms this implies, for equal rheology, that breakthrough velocities will be smaller at larger test scales.

Velocities in the central upwell of the cavern were also measured directly using clay simulant in the 336 and APEL test vessels. In these tests, upwell velocity was measured at various elevations for a given PJM velocity. As the PJMs were operating, upwell velocities oscillated between low and high values as the pulse formed, stabilized, and then diminished. The maximum velocity for each PJM drive was determined, and the average over many cycles was calculated. These data confirmed the general trend that upwell velocity increases with increasing yield Reynolds number.

CONCLUSION

Normalized cavern heights were found to be an increasing function of the yield Reynolds number. Although the data have a degree of scatter, cavern heights were generally found to decrease at smaller scales. This behavior is consistent with the reduction in jet Reynolds number associated with smaller test scales. Surface breakthrough velocity tests performed in both clay and Laponite also showed the yield Reynolds number (based on breakthrough velocity) increased with the test scale factor. Upwell velocity measurements indicated normalized velocities generally decreased with yield Reynolds number. While it was difficult to conclusively observe jet Reynolds number effects, the data suggest that upwell velocities are a weak, decreasing function of jet Reynolds number. The role of Strouhal number was not explicitly examined in the tests since, at equivalent operating conditions, the Strouhal number is independent of scale.

The scaling theory and experimental test results obtained from these tests demonstrate the mixing per-formance of PJM systems in non-Newtonian slurries can be conservatively assessed at reduced scale for the following reasons:

- The three most important dimensionless parameter groups are the Strouhal number, the yield Reynolds number, and the jet Reynolds number. If these parameters are preserved at reduced scale, the essential behavior of the mixing phenomena will be the same as at full scale.

- The Strouhal number, which takes into account unsteady PJM operation, is the same at reduced and full scale when the PJM cycling is reduced by the geometric scale factor.

- The yield Reynolds number, which determines cavern formation due to non-Newtonian fluid behavior, is the same at reduced and full scale when rheology and PJM velocities are the same at both scales.

- The jet Reynolds number, which determines the flow regime (laminar or turbulent), the degree of turbulence, and the magnitude of mixing velocities, will be decreased by the geometric scale factor at reduced scale when rheology and PJM velocities are the same at both scales. This is conservative because full-scale mixing will always occur at higher jet Reynolds number and therefore have a higher degree of turbulence.

REFERENCES

1. Gauglitz, P. A., Rassat, S. D., Bredt, P. R., Konynenbelt, J. H., Tingey, J. M., and Mendoza, D. P. 1996. *Mechanisms of Gas Bubble Retention and Release: Results for Hanford Waste Tanks 241-S-102 and 241-SY-103 and Single-Shell Tank Simulants.* PNNL-11298, Pacific Northwest National Laboratory, Richland, Washington.

2. Enderlin, C. W., Dodson, M.G., Nigl, F., Bontha, J., and Bates, J. M. 2003. *Results of Small-Scale Particle Cloud Tests and non-Newtonian Fluid Cavern Tests*. WTRPT-078 Rev. 0 (PNWD-3360), Battelle – Pacific Northwest Division, Richland, Washington.

3. Meyer, P. A., Kurath, D. E., and Stewart, C. W. 2005. *Overview of the Pulse Jet Mixer Non-Newtonian Scaled Test Program.* WTP-RPT-127 Rev. 0, Battelle – Pacific Northwest Division, Richland, Washington

4. Poloski, A. P., Meyer, P. A., Jagoda, L. K., and Hrma, P. R. 2004. *Non-Newtonian Slurry Simulant Development and Selection for Pulsed Jet Mixer Testing*. WTP-RPT-111 Rev 0 (PNWD-3495), Battelle – Pacific Northwest Division, Richland, Washington.

5. Russell, R. L., Rassat, S. D., Arm, S. T., Fountain, M. S., Hatchell, B. K., Stewart, C. W., Johnson, C. W., Meyer, P. A., and Guzman-Leong, C. E. 2005. *Final Report: Gas Retention and Release in Hybrid Pulse Jet-Mixed Tanks Containing non-Newtonian Waste Simulants*. WTP-RPT-114 Rev. 1 (PNWD-3552), Battelle – Pacific Northwest Division, Richland, Washington.

6. Bamberger, J. A., Meyer, P. A., Bontha, J. R., Enderlin, C. W., Wilson, D. A., Poloski, A. P., Fort, J. A., Yokuda, S. T., Smith, H. D., Nigl, F., Friedrich, M., Kurath, D. E., Smith, G. L., Bates, J. M., and Gerber, M. A. 2005. *Technical Basis for Testing Scaled Pulse jet Mixing Systems for non-Newtonian Slurries*. WTP-RPT-113 Rev. 0 (PNWD-3551), Battelle – Pacific Northwest Division, Richland, Washington.

7. Bates, J.M., Brothers J. W., Alzheimer, J. M., and Wallace D. E. 2004. *Test Results for Pulse Jet Mixers in Prototypic Ultrafiltration Feed Process and High-Level Waste Lag Storage Vessels*. WTP-RPT-110 Rev. 0 (PNWD-3496), Battelle – Pacific Northwest Division, Richland Washington.

8. Rajaratnam, N. 1976. *Turbulent Jets*. Elsevier Science Publishers, New York.

9. Rushton, J. H. 1980. "The Axial Velocity of a Submerged Axially Symmetrical Fluid Jet." *AIChE Journal*, 26(6):1038-1041.

10. Wilson, D. A., Restivo, M. L., Guerrero, H. N., Steeper, T. J., Eibling, R. E., Hansen, E. K., Jones, T. M., and Eberl, K. R. November 2004. *One-Eighth-Scale Pulse Jet Mixer (PJM) - Design Parameters Scale Law Testing*. WSRC-TR-2004-00430 Rev. 0 (SRNL-RPP-2004-00069 Rev. 0), Westinghouse Savannah River Company, Aiken, South Carolina.